Available online www.jocpr.com

Journal of Chemical and Pharmaceutical Research, 2014, 6(7):2470-2476

Research Article

ISSN : 0975-7384
CODEN(USA) : JCPRC5

Kinematics analysis and design of a novel spherical orthogonal 3-RRR parallel mechanism

Liang Zhang[1,2], Zhenlin Jin[1] and Shuzhen Li[2]

[1]College of Mechanical Engineering, Yanshan University, Qinhuangdao, China
[2]College of Mechanical and Electronic Engineering, Hebei Normal University of Science & Technology, Qinhuangdao, China

---

ABSTRACT

A new orthogonal spherical three degrees of freedom (3-DOF) parallel mechanism was presented, and its kinematics performance was analyzed. The position equations and kinematics transmission equations were given by the relation of geometry. Based on the Lagrange method, the evaluation indices of the velocity performance and isotropy performance were defined. The motion characteristics of the mechanism were analyzed, and the distribution of performance indices of the mechanism in task space was studied. The results show that, in the workspace, the range of the velocity performance index is from 0.69157 to 0.96569, the range of isotropic index is from 0.44710 to 0.91281, and the variations of two kinematics transmission performance indices in the working space are small and uniform distribution, so the performance stability of the mechanism within the workspace is good, and the mechanism has good kinematics transmission performance and isotropy performance. With the mechanism for the prototype, a shoulder joint of humanoid robot is developed. It has the advantages of simple and compact structure, easy manufacturing, and lower motion inertia, etc. It is an ideal shoulder joint configuration for the humanoid robot.

Keywords: parallel mechanism, kinematics, performance index, isotropy.

INTRODUCTION

The limited-DOF (degrees of freedom) parallel mechanisms both maintain the inherent advantages of parallel mechanisms and possess several other advantages in terms of simple structure, low cost in manufacturing and operations, therefore they have a potentially wide range of applications [1]. Spherical 3-DOF parallel mechanism is a limited-DOF parallel mechanism which can be widely used for different kinds of practical applications, such as motion simulator, bionic joint and machine tools. So it is attracting the attention of the various researchers. Many prototypes based on spherical 3-DOF parallel manipulator have been developed, such as agile eye [2], NC rotary table [3], wrist joint[4], shoulder joint [5], waist joint [6], and bionic eye [7], etc.

It can be implemented by reasonable design of mechanism layout pattern to improve the performance of parallel mechanism. So the new layout of mechanism design is an important part of the study of parallel mechanism. And the kinematics analysis is the premise and foundation for mechanism design of robot [8,9]. In this paper, a novel parallel 3-RRR orthogonal spherical parallel mechanism is presented. It has such priories as compact structure and low inertia. The position equations and kinematics transmission equations are given by the relation of geometry, and the evaluation indices of the velocity performance and isotropy performance are defined. The motion characteristics of the mechanism are analyzed based on the Lagrange method, and the distribution of performance indices of the mechanism in task space is studied. The study provides the theoretical base for application of the spherical mechanism.

EXPERIMENTAL SECTION

Description of the Novel 3-RRR Parallel Mechanism

The 3-DOF parallel mechanism in the study is a novel parallel 3RRR orthogonal spherical parallel mechanism which is a variation of general 3-RRR spherical parallel mechanism (as shown in Fig.1), the diagram of mechanism is shown in Fig.2. It consists of a fixed platform, a moving platform, and three limbs which consist of a framed link and a connecting rod with identical structure. Each limb connects the fixed platform to the moving platform by three R joints. Thus, the moving platform is attached to the fixed platform by three identical RRR linkages. The connecting rod of the branch near fixed platform is called the frame connecting rod, and the branch close to the moving platform branch is called connecting rod. Each chain consists of three revolute joints in series. Nine revolute axes of the mechanism intersect at one point O, which is the center of rotation of the spherical body. So any point on the movable member of the parallel mechanism is confined in the sphere. The axes of three revolute joints connected with the fixed platform are vertical each another, and the axes of three revolute joints connected with the moving platform are vertical each another, and the revolute joint axes of framed links and connecting rods are vertical each another. So the parallel mechanism possesses advantages in terms of compact structure, easy processing and manufacturing and so on.

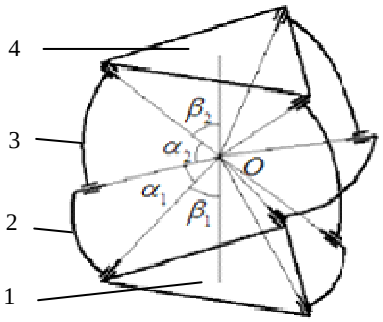

Fig.1 The general spherical parallel mechanism

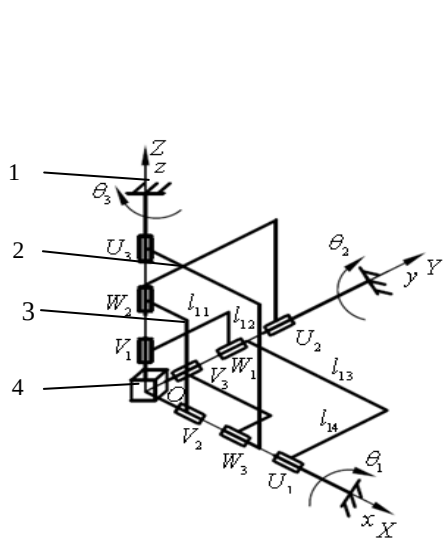

Fig.2 Sketch map of orthogonal spherical parallel mechanism

Kinematics Analysis

To facilitate the analysis, as shown in Fig.2, we assign a fixed Cartesian frame O{X, Y, Z} connected with the fixed platform, and a moving Cartesian frame O{x, y, z} connected with the moving platform at the centered point O, with the X, Y, Z axes in coincidence with $\boldsymbol{U_1, U_2, U_3}$ axes, and the x, y, z axes in coincidence with $\boldsymbol{V_1, V_2, V_3}$ axes, respectively. In the initial posture, the fixed Cartesian frame is coincident with the moving Cartesian frame.

The moving platform only can rotate round the fixed platform, so the method of Z-Y-X Euler angle description is used to describe the transformation matrix between the motion coordinate and the fixed coordinate. Referring to [1], the transformation matrix is given as follows:

$$\boldsymbol{R} = R_{ZYX}(\alpha,\beta,\gamma) = R(Z,\alpha)R(Y,\beta)R(X,\gamma) =$$

$$\begin{bmatrix} \cos\alpha\cos\beta & \cos\alpha\sin\beta\sin\gamma-\sin\alpha\cos\gamma & \cos\alpha\sin\beta\cos\gamma+\sin\alpha\sin\gamma \\ \sin\alpha\cos\beta & \sin\alpha\sin\beta\sin\gamma+\cos\alpha\cos\gamma & \sin\alpha\sin\beta\cos\gamma-\cos\alpha\sin\gamma \\ -\sin\beta & \cos\beta\sin\gamma & \cos\beta\cos\gamma \end{bmatrix} \quad (1)$$

Where the α, β and γ are the posture angles of the moving platform.

Given a set of posture angles (α, β, γ) of the mobile platform, the representation of vector from the moving frame to the fixed frame can be solved by the kinematics analysis. In view of Eq.1, we can derive that

$$\boldsymbol{V_i} = \boldsymbol{R}\boldsymbol{v}_i \tag{2}$$

Where $i = 1$, 2, and 3. Matrix $\boldsymbol{R}$ is the 3×3 rotation or orientation matrix. $\boldsymbol{V}_i$ and $\boldsymbol{v}_i$ is the coordinate of axis in the fixed frame and the moving frame respectively,

When input angle of motor is $\boldsymbol{\theta}_i$, the vector of the corresponding branched intermediate axis $\boldsymbol{W}_i$ relative to the fixed coordinate is given by

$$\boldsymbol{W}_1 = (0 \ \cos\theta_1 \ -\sin\theta)^{\mathrm{T}}$$
$$\boldsymbol{W}_2 = (-\sin\theta_2 \ \ 0 \ \ \cos\theta_2 \ )^{\mathrm{T}}$$
$$\boldsymbol{W}_3 = (\cos\theta_3 \ -\sin\theta_3 \ \ 0)^{\mathrm{T}}$$

The intermediate shaft $\boldsymbol{W}_i$ of branch connects the shaft $\boldsymbol{V}_i$ of the corresponding moving platform through a connecting rod, referring to [1], the constraint equation for the mechanism can be written as follows:

$$\boldsymbol{W}_i \cdot \boldsymbol{V}_i = \cos\alpha \tag{3}$$

Where α is the structure angle of the rods.

Differentiating the constraint equation with respect to time, we can obtain

$$\boldsymbol{A}\dot{\boldsymbol{\theta}} + \boldsymbol{B}\dot{\boldsymbol{\psi}} = \boldsymbol{0} \tag{4}$$

Where $\dot{\boldsymbol{\theta}} = \left(\dot{\theta}_1 \quad \dot{\theta}_2 \quad \dot{\theta}_3\right)^{\mathrm{T}}$ is the vector of actuated joint rates, and $\dot{\boldsymbol{\psi}} = \left(\dot{\alpha} \quad \dot{\beta} \quad \dot{\gamma}\right)^{\mathrm{T}}$ is the vector of the output angular velocities of the mechanism.

$$\boldsymbol{A} = \begin{bmatrix} a_1 & b_1 & c_1 \\ a_2 & b_2 & c_2 \\ a_3 & b_3 & c_3 \end{bmatrix}, \quad \boldsymbol{B} = \begin{bmatrix} d_1 & e_1 & f_1 \\ d_2 & e_2 & f_2 \\ d_3 & e_3 & f_3 \end{bmatrix}$$

Removed the zero elements of A matrix, other elements are expressed as

$$\begin{cases} a_1 = -(\sin\alpha\sin\beta\cos\gamma - \cos\alpha\sin\gamma)\sin\theta_1 - \cos\beta\cos\gamma\cos\theta_1 \\ b_2 = \cos\alpha\cos\beta\cos\theta_2 - \sin\beta\sin\theta_2 \\ c_3 = -(\cos\alpha\sin\beta\sin\gamma - \sin\alpha\cos\gamma)\sin\theta_3 - (\sin\alpha\sin\beta\sin\gamma + \cos\alpha\cos\gamma)\cos\theta_3 \end{cases} \tag{5}$$

Elements in the matrix B are expressed as

$$\begin{cases} d_1 = \cos\theta_1 \cos\alpha \sin\beta \cos\gamma + \cos\theta_1 \sin\alpha \sin\gamma \\ e_1 = \cos\theta_1 \sin\alpha \cos\beta \cos\gamma + \sin\theta_1 \sin\beta \cos\gamma \\ f_1 = -\cos\theta_1 (\cos\alpha \cos\gamma + \sin\alpha \sin\beta \sin\gamma) + \sin\theta_1 \cos\beta \sin\gamma \\ d_2 = -\sin\theta_2 \sin\alpha \cos\beta \\ e_2 = -\cos\alpha \sin\beta \sin\theta_2 + \cos\theta_2 \cos\beta \\ f_2 = 0 \\ d_3 = -\cos\theta_3 \sin\alpha \sin\beta \sin\gamma - \cos\theta_3 \cos\alpha \cos\gamma - \sin\theta_3 \cos\alpha \sin\beta \sin\gamma + \sin\theta_3 \sin\alpha \cos\gamma \\ e_3 = \cos\theta_3 \cos\alpha \cos\beta \sin\gamma - \sin\theta_3 \sin\alpha \cos\beta \sin\gamma \\ f_3 = \cos\theta_3 \cos\alpha \sin\beta \cos\gamma + \cos\theta_3 \sin\alpha \sin\gamma - \sin\theta_3 \sin\alpha \sin\beta \cos\gamma + \sin\theta_3 \cos\alpha \sin\gamma \end{cases} \quad (6)$$

The following velocity equation can be derived from Eq.(4).

$$\dot{\boldsymbol{\psi}} = \boldsymbol{J}\dot{\boldsymbol{\theta}} \quad (7)$$

Where $\boldsymbol{J}$ is defined as kinematics transmission matrix, which relates actuated joint rates to output velocities.

$$\boldsymbol{J} = -\boldsymbol{B}^{-1}\boldsymbol{A} \quad (8)$$

Evaluation Index of the Kinematics

In view of Eq.7, the relationship between input and output of the parallel mechanism motion depends on the matrix $\boldsymbol{J}$. Taking two-norm for Eq.7, we can obtain

$$\left\|\dot{\boldsymbol{\psi}}\right\|^2 = \dot{\boldsymbol{\theta}}^T \boldsymbol{J}^T \boldsymbol{J}\dot{\boldsymbol{\theta}} \quad (9)$$

Assume that the input vector is a unit vector, then

$$\left\|\dot{\boldsymbol{\theta}}\right\| = \dot{\boldsymbol{\theta}}^T \dot{\boldsymbol{\theta}} = 1 \quad (10)$$

Lagrange Multiplier is introduced, and Lagrange equation (11) is constructed by Eq.7.

$$L = \dot{\theta}^T J^T J\dot{\theta} - \lambda\left(\dot{\theta}^T \dot{\theta} - 1\right) \quad (11)$$

The extreme conditions for terminal velocity is expressed as

$$\frac{\partial L}{\partial \dot{\theta}} = 0: \quad J^T J\dot{\theta} - \lambda\dot{\theta} = 0 \quad (12)$$

The extreme for terminal velocity can be derived from Eq.12, which can be written as

$$k_{v\max} = \left\|\dot{\psi}\right\|_{\max} = \sqrt{\lambda_{\max}} \quad , \quad k_{v\min} = \left\|\dot{\psi}\right\|_{\min} = \sqrt{\lambda_{\min}} \quad (13)$$

Where $\lambda_{\max}$ is the maximum eigenvalue of matrix $J^T J$, and $\lambda_{\min}$ is the minimum eigenvalue of matrix $J^T J$. $\left\|\dot{\psi}\right\|_{\max}$ is the maximum value of the output speed of the tip of this parallel mechanism, and $\left\|\dot{\psi}\right\|_{\min}$ is the minimum value of output speed of the tip of this parallel mechanism. The minimum value output speed of the tip of the parallel mechanism is defined as the velocity index. It is larger, the velocity index is better, and the velocity transmission precision is higher.

The more maximum and minimum values of output speed values are approximate, the isotropy of the velocity transmission of the parallel is better. So Eq.14 is defined as the isotropic index of velocity.

$$k = \left\|\dot{\psi}\right\|_{\min} / \left\|\dot{\psi}\right\|_{\max} \quad (14)$$

Where $0 < k \leq 1$, with the value of k closer to one, the velocity isotropy of the parallel is better, contrarily is worse.

RESULTS AND DISCUSSION

A Case Study

The structural parameters of the mechanism are shown in Table 1.

Tab.1 Structural Parameters of the mechanism

Structural Parameters	Value
$l_{11} = l_{14}$ / mm	90
l_{12} / mm	60
l_{13} / mm	150
rod linear density (kg / m)	0.63
moving platform density (kg / m^3)	2800
posture angle α (deg)	$[-20^\circ, 20^\circ]$
posture angle β (deg)	$[-20^\circ, 20^\circ]$
posture angle γ (deg)	$[-20^\circ, 20^\circ]$

Based on Eqs.(7)-(14), the performance indices atlas of the mechanism in task space can be plotted by a developed MATLAB program. Because of the limited space, the performance atlas of α which has the value of 10 deg, 0 deg, and -10 deg are given, as shown in figures 3 to 5.

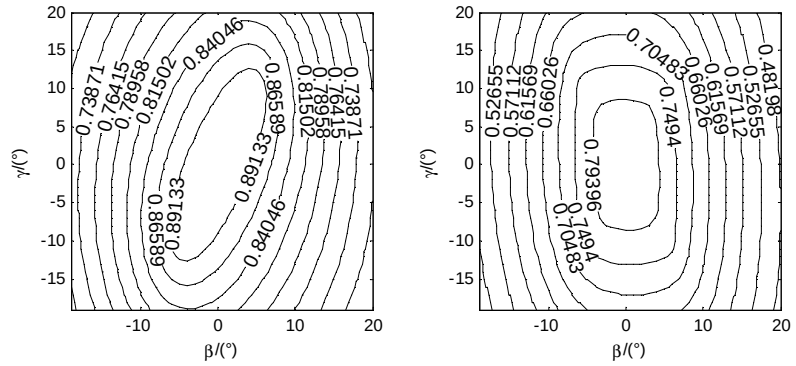

(a) Velocity performance index **(b) Kinematics isotropic index**

Fig. 3 Kinematics performance index distribution in workspace of $\alpha = 10$ deg

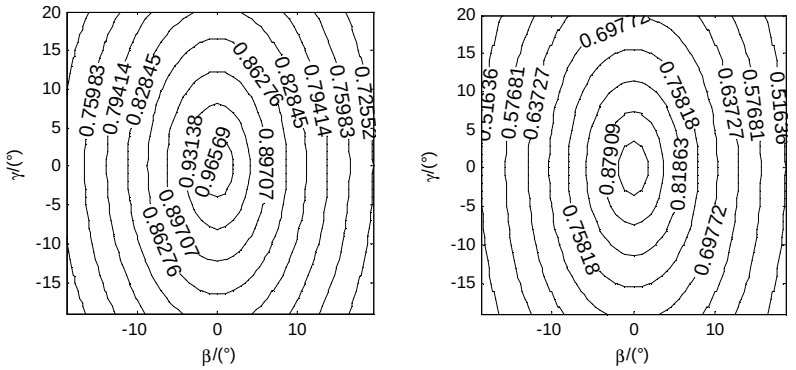

(a) Velocity performance index **(b) Kinematics isotropic index**

Fig. 4 Kinematics performance index distribution in workspace of $\alpha = 0$ deg

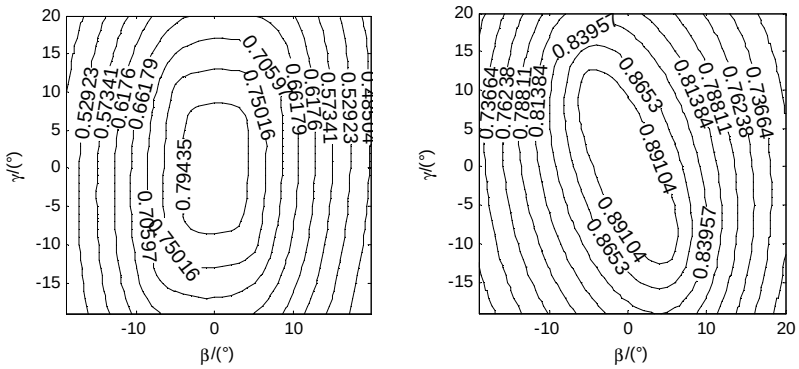

(a) Velocity performance index **(b) Kinematics isotropic index**

Fig. 5 Kinematics performance index distribution in workspace of $\alpha = -10$ deg

The values of kinematics performance index can be derived from Figure 3 to 5 when $\beta \in [-20^{\circ}, 20^{\circ}]$, $\gamma \in [-20^{\circ}, 20^{\circ}]$, and α has the value of 20 deg, 10 deg, 0 deg, -10 deg and -20 deg, as shown in table 2.

In the same way, the values of kinematics performance index can be derived when $\alpha \in [-20^{\circ}, 20^{\circ}]$, $\gamma \in [-20^{\circ}, 20^{\circ}]$, and β has the value of 20 deg, 10 deg, 0 deg, -10 deg and -20deg, as shown in table 3, and when $\alpha \in [-20^{\circ}, 20^{\circ}]$, $\beta \in [-20^{\circ}, 20^{\circ}]$, and γ has the value of 20 deg, 10 deg, 0 deg, -10 deg and -20deg, the values of kinematics performance index are shown in table 4.

Tab.2 Kinematics performance index of（$\beta \in [-20^{\circ}, 20^{\circ}], \gamma \in [-20^{\circ}, 20^{\circ}]$）

posture angle α (deg)	velocity performance index	Kinematics isotropic index
20	0.71016-0.81755	0.47656-0.66490
10	0.73871-0.89133	0.48198-0.79396
0	0.75983-0.96569	0.51636-0.87909
-10	0.73664-0.89104	0.48304-0.79435
-20	0.70830-0.81728	0.47894-0.66524

Tab.3 Kinematics performance index of（$\alpha \in [-20^{\circ}, 20^{\circ}], \gamma \in [-20^{\circ}, 20^{\circ}]$）

posture angle β (deg)	velocity performance index	Kinematics isotropic index
20	0.69481-0.71591	0.44710-0.48042
10	0.78272-0.83286	0.59656-0.68852
0	0.83376-0.95250	0.69484-0.91281
-10	0.76788-0.83248	0.61374-0.68883
-20	0.69385-0.71572	0.44858-0.48071

Tab.4 Kinematics performance index of（$\alpha \in [-20^{\circ}, 20^{\circ}], \beta \in [-20^{\circ}, 20^{\circ}]$）

posture angle γ (deg)	velocity performance index	Kinematics isotropic index
20	0.69157-0.81658	0.47656-0.66490
10	0.74265-0.89099	0.48341-0.79614
0	0.76750-0.93357	0.51563-0.87891
-10	0.74109-0.89077	0.48620-0.79450
-20	0.70808-0.81631	0.47863-0.66519

Summary

(1) The amplitude changes of two kinds of kinematics performance indexes are small and uniform distribution in the workspace, and the values vary with the changing of the mechanism posture, but the performance indexes do not change much. This indicates that the performance stability of the mechanism is better.

(2) Kinematics performance index shows a good symmetry in the working space. At the original position, velocity performance index and isotropic index are approximately equal to 1, this indicates that the speed performance is the best, motion transfer ability is the strongest, speed transmission is isotropic, and the kinematics performance index is the best.

(3) In workspace, the value of velocity performance index ranges from 0.69157 to 0.96569, the value of isotropic index of velocity ranges from 0.44710 to 0.91281, both performance indexes do not exist in the case of zero, so the kinematics transmission performance and isotropic of the mechanism are good. The results are an important base of reference for the design of this parallel mechanism.

Based on the above analysis, and considering the processing and assembly technology, a shoulder joint is designed, as shown in Fig.6. The drivers are fixed on the fixed parts. The fixed drivers make it possible that the moving components of the shoulder joint do not bear any loads of the driver. This enables large powerful drivers to drive relatively small structures. With respect to the series shoulder joint, the shoulder possesses the advantages of compact structure, bearing ability, and low inertia. It is suitable for the humanoid robot fields.

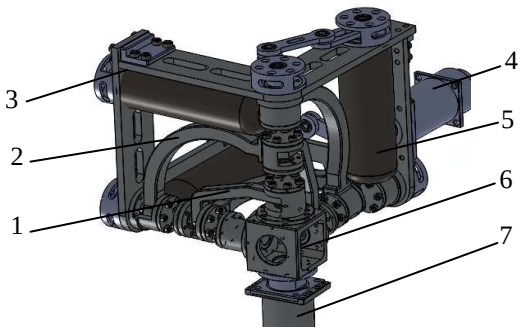

1 connecting rod 2 frame link 3 frame 4 Trunk connector 5 actuator 6 moving platform 7 big arm
Fig.6 Structure of shoulder joint

REFERENCES

[1] Z Huang; YS Zhao; TS Zhao. Advanced Spatial Mechanism, 1st Edition,China Higher Education Press, Beijing, **2006**; 89-201.
[2] CM Gosselin. *Int. J. of Robotic Research,* **1997, 16(5), 619-630.**
[3] XJ Zeng; T Huang; ZP Zeng; et al. *Journal of Machine Design,* **2001,1(4), 13-16.**
[4] LN Sun; Y Liu; YH Zhu. *China Mechanical Engineering,* **2003, 14(10), 831-834.**
[5] YB Li; ZL Jin. *Optics and Precision Engineering,* **2007, 15(5),730-735.**
[6] ZL Jin; Y Rong. *China Mechanical Engineering,* **2007, 18(22): 2697-2700.**
[7] C LI; SR Xie; HY Li; et al. *Robot,* **2010, 32(6), 781-786.**
[8] JF Hu; XM Zhang. *Optics and Precision Engineering,* **2012, 20(12), 2686-2695.**
[9] YB LI, Y Liu; ZF Zhao; et al. *Transactions of the Chinese Society of Agricultural Engineering,* **2013,29(2), 17-23.**